Bifunctional FePt Core−Shell and Hollow Spheres: Sonochemical Preparation and Self-Assembly

Junzhong Wang,[†] Kian Ping Loh,*[,†] Yu Lin Zhong,[†] Ming Lin,[‡] Jun Ding,[#] and Yong Lim Foo[‡]

Department of Chemistry, National University of Singapore, 3 Science Drive 3, Singapore 117543, Department of Materials Science & Engineering, National University of Singapore, Singapore 119620, and Institute of Material Research and Engineering, 3 Research Link, Singapore 117602.

Received February 6, 2007. Revised Manuscript Received March 16, 2007

The sonochemical preparation of $FePt/SiO_2$ and $FePt/ZnS/SiO_2$ core−shell and hollow microspheres, as well as their self-assembly into a quasi-monolayer, was demonstrated. Uniform FePt nanoparticles can be deposited on silica microspheres modified with polyelectrolytes by a sonochemical process, using iron and platinum acetylacetonates as metal precursors. The amine and carboxylic functional groups in the polyelectrolyte layer provided nucleation sites for FePt nanoparticles. Alternatively, if the silica was precoated with ZnS, the nucleation of FePt nanoparticles on the ZnS shell can occur. A high coercivity of 12 kOe for these microspheres was obtained after annealing. A bifunctional microsphere with both luminescence and magnetic properties could be generated after the $FePt/ZnS/SiO_2$ microsphere was annealed in a vacuum.

Introduction

Core−shell and hollow colloidal particles can find many applications[1−4] in areas such as photonic crystals,[2] catalysts,[3] and biotechnology.[4] Among them, magnetic core−shell and hollow capsules have received growing attention due to a variety of biomedical applications such as separation, cancer detection, and drug delivery system by noncontact magnetically guided transport.[1,4,5] The strategy of using silica or polymer as a templating core, followed by nucleation and growth of a shell, allowed a hollow sphere to be generated after selective removal of the core by etching, dissolution, or thermal decomposition.[1] In the context of magnetism, a magnetic hollow sphere can show several unique aspects compared to the flat thin films.[1,6,7] A hollow sphere can maintain single-domain behavior at a much larger diameter than a solid sphere.[6] There is also anisotropic distribution of magnetization due to the curved surface and a decrease in magnetic switching field if the direction of the external magnetic field is applied to the sphere at oblique angles.[7]

Hard magnetic FePt has attracted considerable attention due to its high magnetocrystallinity (Ku, $\sim 6.6 \times 10^7$ erg/cm^3) and magnetic anisotropy. Self-assembled FePt magnetic nanoparticles offer the potential to store data at areal densities >1 Tbit/inch^2. Thin films of these therefore can be engineered for applications in high-density data storage,[8,9] permanent magnets,[10] and biomedicine.[11] However, the magnetic properties of FePt nanoparticles depend critically on the preparation processes, which can determine the final shape and size distribution of the nanoparticles. Elkins[12] reported the chemical reduction of $Pt(acac)_2$ and $Fe(acac)_3$ by 1,2-hexadecanediol at $\sim$295 °C in solution phase to obtain monodisperse FePt nanoparticles with sizes between 2 and 4 nm. Jeyadevan[13] reported the reduction of iron and platinum acetylacetonates by ethylene glycol in 200 °C, and partly ordered fct phase of FePt could be obtained. Heat treatment is required to induce phase transformation from

* Corresponding author. E-mail: chmlohkp@nus.edu.sg.
[†] Department of Chemistry, National University of Singapore.
[‡] Department of Materials Science & Engineering, National University of Singapore.
[#] Institute of Material Research and Engineering.

(1) (a) Wilcox, D. L.; Berg, M.; Bernat, T.; Kellerman, D.; Cochran, J. K., Jr. *Mater. Res. Soc. Symp. Proc.* **1994**, *372*, 1. (b) Caruso, F. *Adv. Mater.* **2001**, *13*, 11.
(2) (a) Joannopoulos, J. D.; Villeneuve, P. R.; Fan, S. *Nature* **1997**, *386*, 143. (b) Rogach, A.; Susha, A.; Caruso, F.; Sukhorukov, G.; Kornowski, A.; Kershaw, S.; Möhwald, H.; Eychmüller, A.; Weller, H.; *Adv. Mater.* **2000**, *12*, 333. (c) Xu, X. L.; Asher, S. A. *J. Am. Chem. Soc.* **2004**, *126*, 7940.
(3) (a) Chen, C. W.; Chen, M. Q.; Serizawa, T.; Akashi, M. *Chem. Commun.* **1998**, 831. (b) Caruso, F.; Fiedler, H.; Haage, K. *Colloids Surf., A* **2000**, *169*, 287.
(4) (a) Velev, O. D.; Jede, T. A.; Lobo, R. F.; Lenhoff, A. M. *Nature* **1997**, *389*, 447. (b) Holland, B. T.; Blanford, C. A.; Stein, A. *Science* **1998**, *281*, 538. (c) Marinakos, S. M.; Shultz, D. A.; Feldheim, D. L. *Adv. Mater.* **1999**, *11*, 34.
(5) (a) Caruso, F.; Spasova, M.; Susha, A.; Giersig, M.; Caruso, R. A. *Chem. Mater.* **2001**, *13*, 109. (b) Arruebo, M.; Galan, M.; Navascues, N.; Tellez, C.; Marquina, C.; Ibarra, M. R.; Santamaria, J. *Chem. Mater.* **2006**, *18*, 1911.
(6) (a) Goll, D.; Berkowitz, A. E.; Bertram, H. N. *Phy. Rev. B* **2004**, *70*, 184432. (b) Ulbrich, T. C.; Makarov, D.; Hu, G.; Guhr, I. L.; Suess, D.; Schrefl, T.; Albrecht, M. *Phy. Rev. Lett.* **2006**, *96*, 077202−1. (c) Beleggia, M.; Lau, J. W.; Schofield, M. A.; Zhu, Y.; Tandon, S.; De Graef, M. *J. Magn. Magn. Mater.* **2006**, *301*, 131.
(7) (a) Deng, Y. J.; Blote, H. W. J. *Phy. Rev. E* **2003**, *67*, 066116. (b) Pleimling, M. *J. Phys. A: Math Gen.* **2004**, *37*, R79. (c) Liu, W. M.; Wang, X. B.; Pu, F. C.; Huang, N. N. *Phys. Rev. E* **1997**, *55*, 1375.
(8) Sun, S. *Adv. Mater.* **2006**, *18*, 393.
(9) Sun, S.; Murray, C. B.; Weller, D.; Folks, L.; Moser, A. *Science* **2000**, *287*, 1989.
(10) Zeng, H.; Li, J.; Wang, Z. L.; Liu, J. P.; Sun, S. *Nature* **2002**, *420*, 395.
(11) Pankhurst, Q. A.; Connolly, J.; Jones, S. K.; Dobson, J. *J. Phys. D: Appl. Phys.* **2003**, *36*, R167.
(12) Elkins, K. E.; Vedantam, T. S.; Liu, J. P.; Zeng, H.; Sun, S.; Wang, Z. L.; Ding, Y. *Nano Lett.* **2003**, *3*, 1647.
(13) Jeyadevan, B.; Hobo, A.; Urakawa, K.; Chinnasamy, C. N.; Shinoda, K.; Tohji, K. *J. Appl. Phys.* **2003**, *93*, 7574.

10.1021/cm0703728 CCC: $37.00
Published on Web 04/17/2007

Scheme 1. Schematic Illustration of Sonochemical Preparation of FePt Core−Shell Spheres and the Self-Assembly of the FePt Microsphere Monolayer (PEI, poly(ethyleneimine); PAA, Poly(acrylic acid))

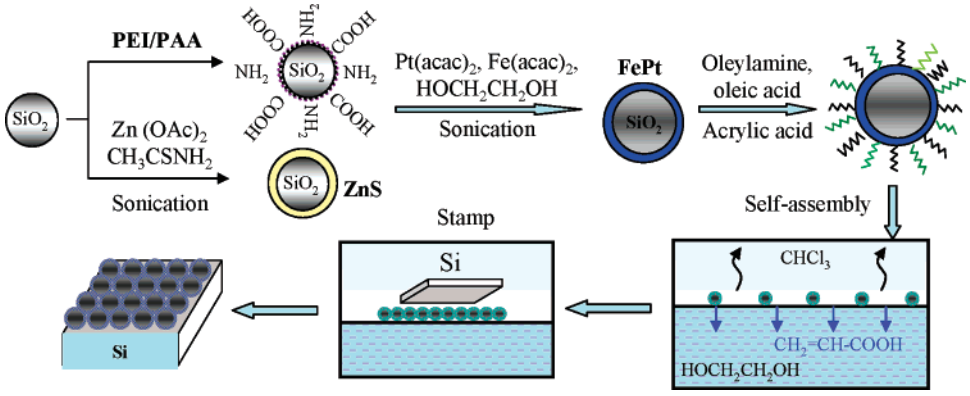

fcc to the hard magnetic fct phase. The coalescence of FePt nanoparticles during annealing can be prevented by coating the FePt nanoparticles (such as FePt/Fe_3O_4,[14] FePt/SiO_2,[15] FePt/MnO[16]) with oxide matrix. Recently, Salgueiriñ-Maceira[17] reported the adsorption of FePt nanoparticles on silica sphere via electrostatic attraction; however, the magnetic properties of these adducts were not investigated. FePt nanocomposites, such as FePt−CdS[18] and FePt−ZnS[19] bimodal nanoparticles, have recently been investigated to act as bifunctional nanoparticles showing dual properties of magnetism and luminescence. These properties are potentially useful in biomedicine, although one issue may be the quenching of luminescence by FePt in the case of CdS in core−shell FePt/CdS.[20]

High-intensity ultrasound has become a useful tool to synthesize a number of nanosize materials[21−25] including core−shell[23,24] and hollow spheres.[25] Acoustic cavitation can produce hot spots (instantaneous ∼5000 K, ∼1000 atm, and quenching rates above 1×10^{10} K/s) and unusual physical and chemical effects.[22,26] Very recently, FePt nanoparticles with high coercivity were prepared by ultrasonically assisting decomposition of synthesized precursor $Pt_3Fe_3(CO)_{15}$.[27] In this work, surface chemistry was applied to modify the interface between FePt and the silica microsphere so that the nucleation of the FePt on the surface-modified silica can be achieved. Finally, we investigated the possibility of generating a bifunctional magnetic−luminescent microsphere.

Experimental Section

Materials and Instruments. Chemicals (Aldrich) were purchased from Sigma-Aldrich, Singapore, except for platinum(II) acetylacetonate ($Pt(acac)_2$, 98%, Acrōs Organics) and zinc acetate ($(CH_3COO)_2{\cdot}2H_2O$, Merck). Iron(II) acetylacetonate ($Fe(acac)_2$, 99.95%), iron(III) acetylacetonate ($Fe(acac)_3$, 99.9%), ethylene glycol (99%), thioacetamide (98%), poly(ethyleneimine) (PEI, 50% (w/v) in H_2O, M_w 200 000), poly(acrylic acid) (PAA, M_w 450 000), tetraethyl orthosilicate (99%), ammonia (28−30%). The chemicals were used without further purification.

Ultrasonic irradiation was carried out using a high-intensity ultrasonic probe (Sonics & Materials, VCX-750, 13 mm diameter Ti horn, 20 kHz). The Suslick cell has a diameter of 25 mm. The ultrasonic probe was usually immersed ∼1 cm under the reaction liquid surface, and the amplitude (power) of sonication was controlled at 25−40% of total power output (750 W).

(1) Modification of Silica Spheres. *(a) Deposition of Polyelectrolyte Layers of PEI and PAA using Layer-by-Layer Technique (P2/SiO_2).* Electrostatic attraction is the main driving force for the deposition of positively charged PEI with NH_2 (or NH_3^+) groups and negatively charged PAA with −COOH (or $-COO^-$) groups on the negatively charged surface of the silica template. Silica spheres were synthesized following the Stöber method.[28] The silica particles in water dispersion were deposited by a two-layer polyelectrolyte of aqueous PEI and PAA. Typically, 2 mL of PEI (2 mg/mL, pH was preadjusted to ∼3 by 1.0 mol/mL of HCl) was added into a colloidal dispersion of 0.1 g of silica/30 mL of deionized water, followed by a bath sonication to get a colloidal dispersion. It was then centrifuged and washed by deionized water three times. A similar process was applied to coat PAA (2 mg/mL, pH was adjusted to ∼8 by 1.0 mol/mL of NaOH to have a more negative charge with more $-COO^-$ groups on PAA) on the PEI-coated SiO_2. Finally, the white powder was dried at 60 °C.

(b) ZnS-Coated SiO_2 Core−Shell Sphere (ZnS/SiO_2). Typically, 100 mg of SiO_2 (heated at 180 °C for 12 h in advance) was added into a solution of $Zn(Ac)_2{\cdot}2H_2O$ (600 mg, 2.73 mmol) in 40 mL of deionized water and sonicated for ∼10 min for dispersion.[23] Thioacetamide (205 mg, 2.73 mmol) was then added into the dispersion and sonicated in air for 3 h. The total amount of sonochemical energy delivered to the probe was digitally displayed as $\sim 8 \times 10^{-4}$ J. The resulting white powder was recovered by

(14) Zeng, H.; Li, J.; Wang, Z. L.; Liu, J. P.; Sun, S. *Nano Lett.* **2004**, *4*, 187.
(15) Lee, D. C.; Mikulec, F. V.; Pelaez, J. M.; Koo, B.; Korgel, B. A. *J. Phys. Chem. B* **2006**, *110*, 11160.
(16) Kang, S.; Miao, G. X.; Shi, S.; Jia, Z.; Nikles, D. E.; Harrell, J. W. *J. Am. Chem. Soc.* **2006**, *128*, 1042.
(17) Salgueiriñ-Maceira, V.; Correa-, Duarte, M. A.; Farle, M. *Small* **2005**, *1*, 1073.
(18) Gu, H. W.; Zheng, R. K.; Zhang, X. X.; Xu, B. *J. Am. Chem. Soc.* **2004**, *126*, 5664.
(19) Gu, H. W.; Zheng, R. K.; Liu, H.; Zhang, X. X.; Xu, B. *Small* **2005**, *1*, 402.
(20) Lin, H. Y.; Chen, Y. F.; Wu, J. G.; Wang, D. I.; Chen, C. C. *Appl. Phys. Lett.* **2006**, *88*, 161911.
(21) Flint, E. B.; Suslick, K. S. *Science* **1991**, *253*, 1397.
(22) Suslick, K. S.; Price, G. J. *Annu. Rev. Mater. Sci.* **1999**, *29*, 295.
(23) Dhas, N. A.; Zaban, A.; Gedanken, A. *Chem. Mater.* **1999**, *11*, 806.
(24) Breen, M. L; Dinsmore, A. D.; Pink, R. H.; Qadri, S. B.; Ratna, B. R. *Langmuir* **2001**, *17*, 903.
(25) Dhas, N. A.; Suslick, K. S. *J. Am. Chem. Soc.* **2005**, *127*, 2368.
(26) Suslick, K. S.; Hammerton, D. A.; Cline, R. E. *J. Am. Chem. Soc.* **1986**, *108*, 5641.
(27) Rutledge, R. D.; Morris, W. H.; Wellons, M. S.; Gai, Z.; Shen, J.; Bentley, J.; Wittig, J. E.; Lukehart, C. M. *J. Am. Chem. Soc.* **2006**, *128*, 14210.
(28) Stöber, W.; Fink, A.; Bohn, E. *J. Colloid Interface Sci.* **1968**, *26*, 62.

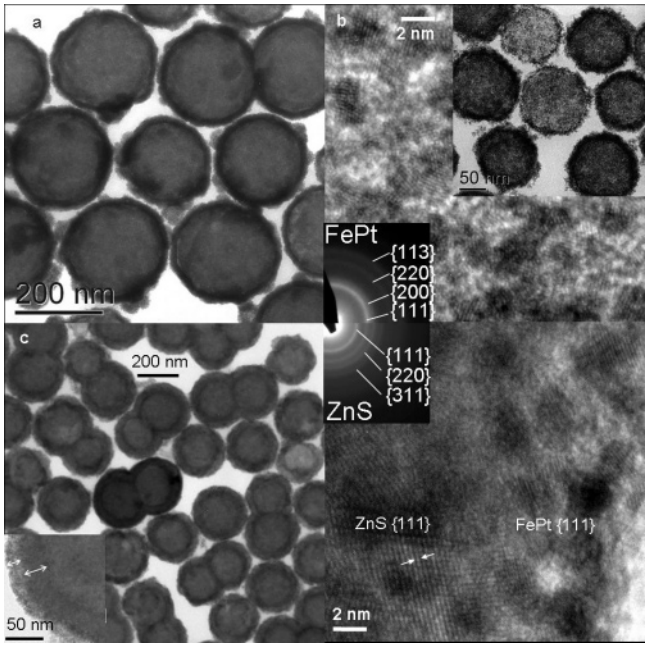

Figure 1. TEM images of fcc phase FePt core−shell spheres: (a) average size ~240 nm FePt/SiO_2 using Fe(III)$(acac)_3$ as iron precursor, (b) HRTEM image of dense 3−5 nm FePt clusters on the FePt/SiO_2 shell (inset, ~120 nm FePt/SiO_2 using Fe(II)$(acac)_2$ as iron precursor, and SAED pattern of FePt shows fcc phase), (c) FePt/ZnS/SiO_2 (inset, the thickness of ZnS shell and FePt shell is ~30 nm and ~15 nm, respectively), (d) HRTEM of FePt and ZnS nanoparticles on the shell (0.312 nm for ZnS {111} plane, 0.227 nm for FePt {111} plane, inset SAED pattern shows fcc FePt and crystalline ZnS).

centrifugation, washed repeatedly with deionized water, and then dried at 60 °C.

(2) Sonochemical Preparation of FePt-Based Core−Shell Sphere (FePt/SiO_2 and FePt/ZnS/SiO_2). Typically, 0.010 g of P2/SiO_2 in 12 mL of ethylene glycol was sonicated for about 10 min to get a colloidal dispersion. Pt$(acac)_2$ (0.060 g) and Fe$(acac)_2$ (0.078 g, or 0.108 g of Fe$(acac)_3$) were then added into the dispersion and sonicated for 2−4 h under an Ar gas flow. (For synthesis of FePt/ZnS/SiO_2, the amounts of ZnS/SiO_2, Pt$(acac)_2$, and Fe$(acac)_2$ added were typically 0.020, 0.985, and 0.127 g, respectively.) During the sonication, the temperature increased to 115 ± 5 °C automatically. The black mixture was centrifuged; the black precipitate was washed several times with ethanol and then dispersed in hexane that contained several drops each of oleic acid and oleylamine, centrifuged, and washed by hexane.

(3) Self-Assembly of FePt Core−Shell Colloidal Particles and Thermal Annealing. The FePt core−shell particles were dispersed and washed by a chloroform solution with ~1 mg/mL of stabilizer, which consists of equivalent amounts of oleic acid and oleylamine. A black chloroform dispersion consisting of 10 mg/mL FePt/ZnS/SiO_2 particles, ~0.1 mL of oleic acid/oleylamine, and ~0.02 g/mL acrylic acid was used for the two-dimensional self-assembly. Several drops of this dispersion were dropped onto the ethylene glycol surface at room temperature. After the evaporation of chloroform from the two-dimensional self-assembly on the ethylene glycol surface, the self-assembled layer was transferred onto the Si substrate by stamping the latter lightly on the surface of the liquid, followed by washing with ethanol. The similar process was applied for the self-assembly of a monolayer of FePt/SiO_2.

The annealing of the film was performed in a vacuum of 1×10^{-9} Torr. Magnetic properties were measured at room temperature using a Lake Shore 7400 vibrating samples magnetometry (VSM) instrument with an applied magnetic field up to 20 kOe and a superconducting quantum interference device (SQUID) with a maximum applied field of 50 kOe. X-ray powder diffraction (XRD) were recorded at a scan rate of 0.01°/s using the *K*α line of copper (1.540600 Å). Transmission electron microscopy (TEM) images were obtained with a JEOL 3010 microscope at an acceleration voltage of 300 kV and JEOL UHV-TEM with a base pressure of $\sim 1 \times 10^{-9}$ Torr. SEM images were taken on JEOL 6701 FESEM (field emission scanning electron microscopy). Photoluminescence (PL) spectra were recorded for the solid samples on the SiO_2/Si substrate with a Renishaw 2000 micro-PL setup equipped with 325 nm excitation from a He−Cd laser. X-ray photoelectron spectroscopy (XPS) was performed with the Phobios 100 electron analyzer, using an unmonochromated Al Kα X-ray source (1486.6 eV).

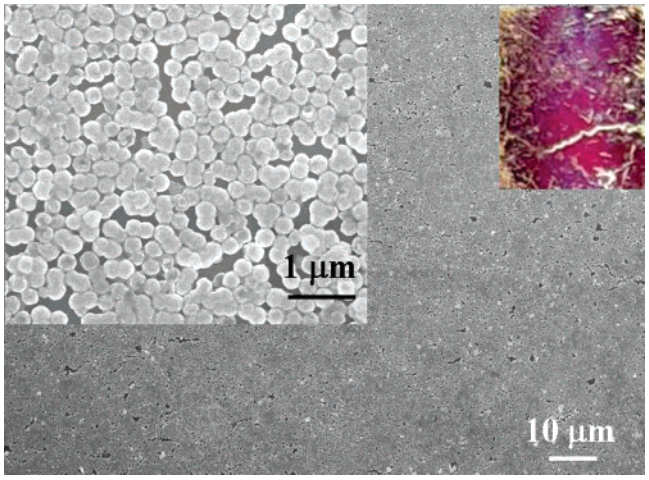

Figure 2. SEM image of a quasi-monolayer of FePt/ZnS/SiO_2 microspheres assembled on Si substrate (left inset, magnified image; right inset, photograph of samples (~5 × 8 mm) scattered in the {111} planes, showing red color reflection).

Results and Discussion

One unique aspect of the current approach is the direct sonochemical reduction of iron and platinum precursors to form FePt nanoparticles in ethylene glycol at a relatively low temperature of 120 °C. No chemical reducing agent such as 1,2-hexadecanediol, or the use of surfactants to stabilize these nanoparticles, is needed. In this case, the sonochemically reduced FePt nanoparticles were deposited directly on the polyelectrolyte-coated spheres. In addition, sonochemistry assists with the uniform coating of FePt on the spherical template by a surface self-cleaning effect; this arises from microjet "sputtering" driven by ultrasonic cavitation.[23−25] To initiate high-density nucleation of FePt uniformly on the silica microsphere, we used amine and carboxylic functional groups to decorate the surface of the silica microsphere by codepositing a polyelectrolyte layer of PEI (poly(ethyleneimine) and PAA (poly(acrylic acid)). It is well-known that FePt has a high affinity for carboxylate and amine groups; for example, surfactant exchange has been used routinely in the literature as a strategy to control the interparticle spacing in FePt nanoparticle assemblies by replacing long-chain oleate and oleylamine with short-chain acid and amine.[8] The COOH group of PEI can covalently bond to Fe, forming iron carboxylate (−COO−Fe) in monodentate fashion, or as chelate ligand to binding with Fe via two O atoms, whereas the amine group, as electrodonor, can bind to Pt via coordination bond.[8] The layered deposition of PEI and PAA can also help to provide a uniform charge distribution

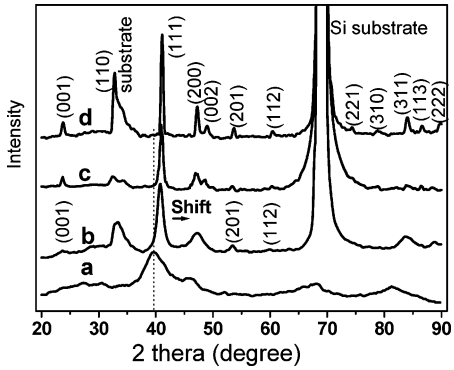

Figure 3. XRD patterns of $FePt/SiO_2$ films on SiO_2/Si substrate annealed for 30 min under a high vacuum (1×10^{-9} Torr): (a) sonochemically prepared powder without annealing; (b) annealed at 400, (c) 500, and (d) 600 °C.

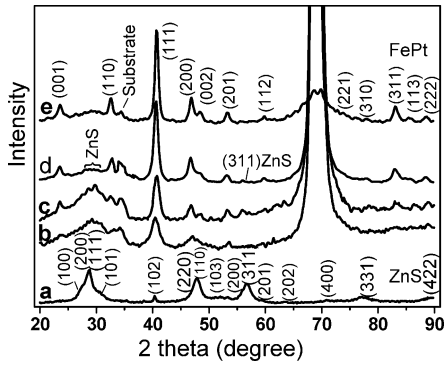

Figure 4. XRD patterns of $FePt/ZnS/SiO_2$ films on SiO_2/Si substrate annealed under a high vacuum for 30 min at different temperatures: (a) ZnS/SiO_2 powder, (b) 450, (c) 500, (d) 530, and (e) 600 °C.

that is useful in the uniform coating of FePt on silica spheres. The thickness of the FePt shell formed can be controlled by adjusting the ratio of FePt precursors and the concentration and size of the silica microsphere used.

Alternatively, a ZnS shell was first synthesized around the silica spheres, and then sonochemical irradiation of platinum and iron acetylacetonates in ethylene glycol was carried out, as shown in Scheme 1. FePt clusters nucleate on the ZnS shell because of the excellent lattice match between the (200) (∼1.93 Å) planes of FePt (JCPDS 43-1359) and the (220) (∼1.91 Å) plane of ZnS (JCPDS 05-0566), as well as the formation of sulfide bonds like Fe−S and Pt−S. Another motivation for selecting ZnS as a component of the double shell is its fluorescence property, which is useful for generating the bifunctional particle in this case.

Our strategy to compress FePt core−shell colloidal particles into a self-assembled film at the air−ethylene glycol interface involves the stabilization of these particles using equivalent volumes of oleic acid and oleylamine in chloroform. A drop of this surfactant-stabilized system was then introduced onto the surface of ethylene glycol. Acrylic acid (CH_2═CH−COOH) was selected as a spreading agent because of its ability to tune the surface stress between the drop of chloroform dispersion and the liquid surface of ethylene glycol. It has a good solubility in ethylene glycol and bonding to Fe of FePt with carboxylic acid group. Following the formation of a self-assembled monolayer of micropheres on the surface, this can be transferred to solid substrate by stamp-transfer.

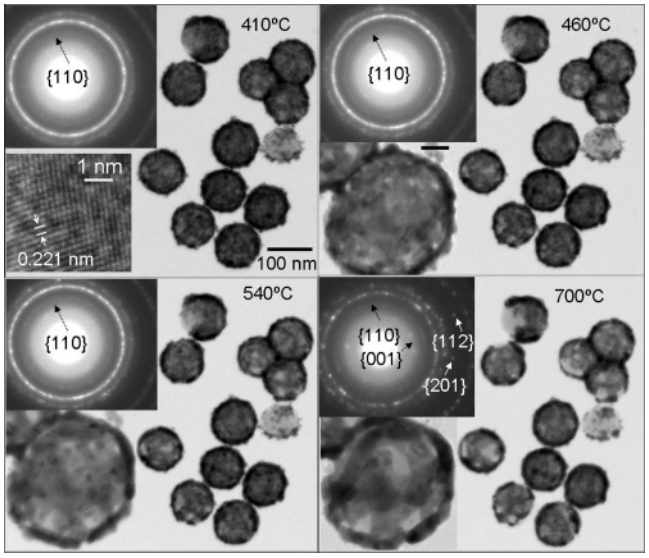

Figure 5. In situ TEM observation of $FePt/SiO_2$ annealed at different temperatures; samples were mounted on silicon-oxide-coated Mo grids and annealed in a vacuum (1×10^{-9} Torr, inset bar is 20 nm).

Figure 1 shows the TEM images of the $FePt/SiO_2$ and $FePt/ZnS/SiO_2$ microspheres. In images b and d of Figure 1, it can be seen that FePt, with a particle size of 3−5 nm, forms a densely packed shell. The crystal lattice (∼0.228 nm) of the FePt cluster and the selected area electron diffraction (SAED) pattern in the inset in Figure 1b indicate that the FePt is fcc phase ({111}, {113}, {200}, {220}).[9] Smaller-sized silica particles typically result in a thinner shell of FePt due to higher surface area presented to the reagents (image a and the inset of image b in Figure 1). A double shell structure was formed around silica in the case of FePt/ZnS, as shown in Figure 1d. The measured *d* spacings are ∼0.312 and ∼0.227 nm, respectively, matching well with the (111) plane of cubic ZnS (JCPDS 05-0566) and (111) plane of fcc FePt. The SAED pattern in the inset confirmed the presence of both phases of crystalline ZnS and fcc FePt. XPS and EDX analysis revealed that the composition of FePt particle is Pt-rich, with 40−47 at % Fe. XPS studies (see the Supporting Information, Figure S1) reveal that the binding energy of Fe2p (711.1 eV) shifts to lower energy (707.5 eV) when $FePt/ZnS/SiO_2$ is annealed at 300 °C, which is probably due to the removal of organic ligands, because the content of carbon is reduced and the binding energy of carbon shifted from 285.1 to 284.7 eV). The photoemission peaks of Zn and S could not be observed before the sample was annealed to 300 °C, indicating the formation of a uniform coating of FePt on the ZnS shell. The Zn and S peaks can be seen clearly following annealing above 300 °C due to clustering of FePt on the ZnS shell, exposing the ZnS underlayer. Annealing to 520 ± 50 °C initiates some evaporation of ZnS from the sample. By 590 °C, the Zn peak vanished completely in the XPS spectrum, whereas the sulfur peak still remained, which suggests the formation of Fe−S and Pt−S bonds. No significant change in the size and composition of the FePt nanoparticles was observed when iron precursors (Fe(II) $(acac)_2$ or Fe(III)$(acac)_3$) with different oxidation states were used.

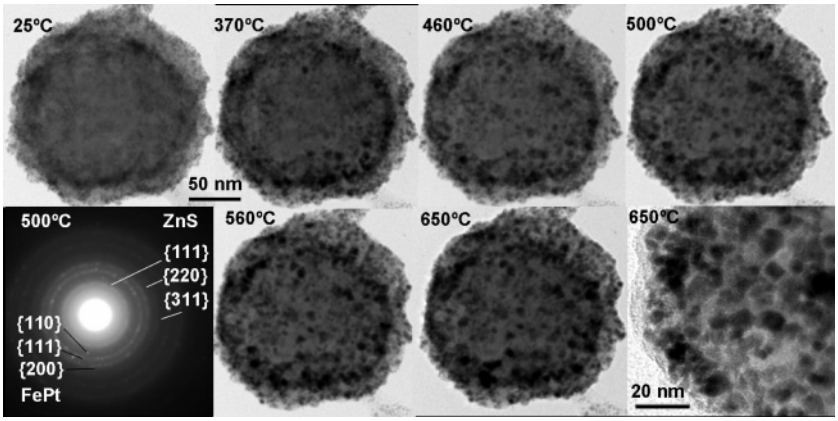

Figure 6. In situ TEM observation of FePt/ZnS/SiO_2 on SiO_x/Mo grids annealed at different temperatures.

As shown in Figure 2, a quasi-monolayer of FePt/ZnS/SiO_2 core−shell microspheres (∼240 nm) can be obtained by a self-assembly process at the air−liquid interface. This is a useful property that allows these FePt microspheres to be manipulated in hydrophilic environment. Interestingly, the monolayer can exhibit a color reflection in the {111} planes, which is related to the interdistance of particles.[29a] The phenomenon indicates that the FePt-nanoparticle-coated silica sphere can be self-assembled to form periodic arrays. Potentially, such types of FePt core−shell microsphere may be developed into magnetic photonic crystal, or undergo architectured assembly to form magnetic superlattices.[29b]

Figure 3 shows XRD patterns of the FePt core−shell spheres before and after annealing at different temperatures. Before annealing, the sonochemically synthesized FePt exhibits a chemically disordered A1-FePt phase (fcc phase, Figure 3a), which is magnetically soft. After annealing at ∼400 °C, a partial $L1_0$-FePt phase (fct phase) starts to develop. It can be seen that (001) and (201) peaks of fct FePt appear and (111) peak shifts to higher angle ($d \approx 0.224$ nm), following an annealing process at ∼400 °C for 30 min. A chemically ordered fct structure (JCPDS 43-1359) that exhibits hard magnetism was obtained when the film was annealed at 600 °C for 30 min (the d value of (111) peak shifts to ∼0.219 nm), as shown in Figure 3d. The narrowing of the XRD peaks with the increase in annealing temperature is indicative of grain growth.

The sonochemically prepared ZnS/SiO_2 powder is a mixture of cubic sphalerite (JCPDS 05-0566) and hexagonal wurtzite (JCPDS 80-0007), as seen in Figure 4a. When the FePt/ZnS/SiO_2 samples were annealed at 450 °C, the partial phase transformation of FePt occurred. XRD analysis of FePt/ZnS/SiO_2 shows that the size of the FePt particle grown on ZnS is smaller than that of FePt/SiO_2 (Figures 3 and 4). The size of the FePt particle could be estimated from Scherrer's equation; it was around 20 nm for FePt/SiO_2 and 10 nm for FePt/ZnS/SiO_2 annealed at 500 °C.

To observe the particle agglomeration process and phase transformation of the FePt nanoparticles on the microsphere, we performed in situ TEM thermal annealing of the FePt under high vacuum conditions, utilizing a heating rate of 10 °C/min. FePt exists in a chemically disordered fcc phase with very small coercitivity and soft magnetism initially and needs thermal annealing to transform it into the chemically ordered fct phase with large coercitivity and hard magnetism. The {001} diffraction spots started to appear at temperatures ranging from 400 to 460 °C. The lattice spacing of the (111) plane after annealing to 410 °C is ∼0.221 nm, which is indicative of the phase transformation from fcc to fct at a relatively low temperature.[30] Diffraction rings ({110}, {001}, {201}, {112}) corresponding to the fct phases become observable at an annealing temperature of 540 °C and became fully developed at 700 °C, as shown in Figure 5. The FePt particles on the shell clustered with increasing annealing temperature, but generally remained stable against evaporation and larger scale aggregation to 700 °C. In situ TEM observation reveals that the ripening of the FePt particle on FePt/ZnS/SiO_2 occurs much more slowly than the FePt/SiO_2 (Figure 6). After annealing to a temperature of 650 °C, the particle size was between 8 and 15 nm, much smaller than that observed for FePt/SiO_2, which was larger than 25 nm. This may be explained by the formation of Fe−S and Pt−S bonds on ZnS, which increased the activation energy for diffusion and aggregation of FePt particle.[31] The onset temperature for FePt phase evolution was also observed to be higher on ZnS.

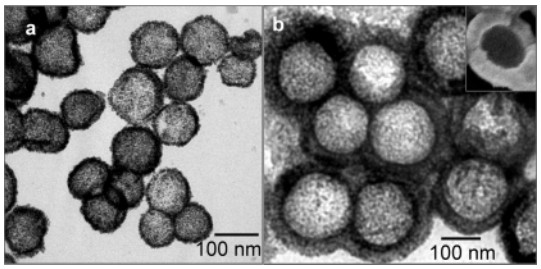

Figure 7. TEM images of hollow spheres derived from the FePt core−shell spheres: (a) hollow FePt, (b) hollow FePt/ZnS double shells (inset, SEM image).

Hollow spherical FePt particles can be obtained when FePt core−shell particles were reacted with 2 wt % HF/ethanol

(29) (a) Gates, B.; Xia, Y. *Adv. Mater.* **2001**, *13*, 1605. (b) Baryshev, A. V.; Kodama, T.; Nishimura, K.; Uchida, H.; M. Inoue, *J. Appl. Phys.* **2004**, *95*, 7336.

(30) Dai, Z. R.; Sun, S.; Wang, Z. L. *Nano Lett.* **2001**, *1*, 443.

(31) Yu, A. C. C.; Mizuno, M.; Sasaki, Y.; Inoue, M.; Kondo, H.; Ohta, I.; Djayaprawira, D.; Takahashi, M. *Appl. Phys. Lett.*, **2003**, *82*, 4352.

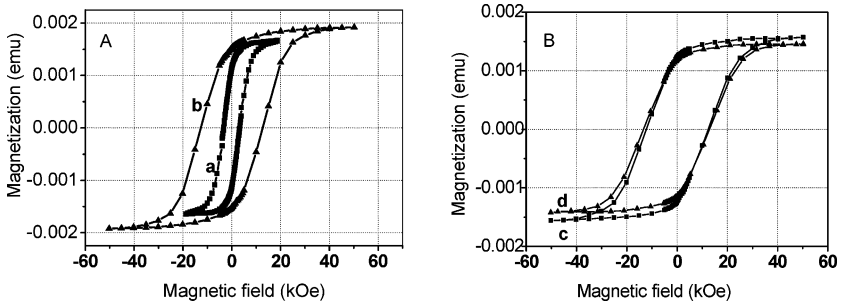

Figure 8. Room-temperature hysteresis loops. (A) FePt/SiO_2: (a) 400 °C for 20 min (■), (b) 600 °C for 10 min (▲). (B) FePt/ZnS/SiO_2 at 530 °C for 30 min: (c) core−shell (■), (d) hollow (▲).

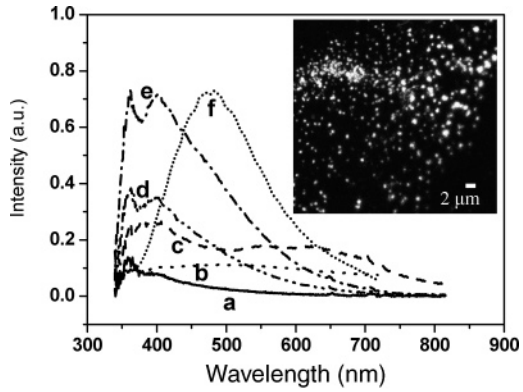

Figure 9. Photoluminescence of FePt/ZnS/SiO_2 film annealed at various temperatures: (a) 400, (b) 500, (c) 530, and (d) 550 °C, reacted with HF/ethanol to remove SiO_2 core, (e) 550 °C, (f) ZnS/SiO_2, for comparison (λ_{ex}= 325 nm). Inset: fluorescence (>500 nm emission) image of (e) using a laser source of 405 nm (Olympus Fluoview FV1000).

to remove the SiO_2 core. The magnetic properties of hollow spheres can be tuned from soft to hard magnetism by controlling the annealing process. Figure 7 shows FePt and FePt/ZnS hollow spheres derived from the etching core−shell spheres annealed at 480 °C under N_2.

The core−shell and hollow particles were transformed into magnetically hard materials after annealing. As seen in Figure 8A, FePt/SiO_2 core−shell particles exhibit coercivity of 3.5 and 12.5 kOe at room temperature when annealed under a high vacuum at 400 °C for 20 min and 600 °C for 10 min for a and b, respectively. These values are comparable to reported work using the same iron precursor.[12,13] The coercivity of hard magnetic FePt/ZnS/SiO_2 is usually higher than FePt/SiO_2 for the same annealing conditions, which may be attributed to the smaller degree of grain coalescence of FePt on ZnS layer.[32] As shown in Figure 8B, the coercivity of the FePt/ZnS/SiO_2 core−shell sample annealed at 530 °C is 12.0 kOe; when the core−shell samples were transformed into hollow shells, the coercivity becomes 12.5 kOe. The removal of nonmagnetic core may improve the magnetic coupling of spherical shells in the self-assembly network.[6b,33]

Although the ZnS/SiO_2 core−shell sample before coating with FePt shows an emission peak centered at ∼480 nm (Figure 9f), the unannealed FePt-coated ZnS/SiO_2 powders shows little luminescence when excited with 325 nm laser radiation, which suggests the quenching of the defect-dominated luminescence by FePt.[20,34] After annealing of the monolayer array in a high vacuum, photoluminescence from the FePt/ZnS/SiO_2 was recovered. One explanation is that quenching by FePt occurs for the defect-dominated green luminescence of ZnS; after annealing, the defect-related sub-gap states were removed and near-band-edge radiation was emitted instead, and the energy transfer between ZnS and FePt was prevented.[35] As shown in Figure 9, emission peaks in UV band was observed for the samples annealed at 400−550 °C for 30 min under a high vacuum and the intensity increased with annealing temperature. The peaks at ∼361 nm (3.43 eV) and ∼402 nm (3.08 eV) may be attributed to near-band-edge emission of wurtzite ZnS.[36] A weak peak at ∼720 nm (1.72 eV) is the first-order harmonic. Figure 9 (inset) shows a confocal micrograph of the microspheres where fluorescence from individual microsphere could be observed. Therefore, the annealing process under a vacuum has the dual role of generating hard magnetism from the core−shell microspheres and recovering fluorescence from the ZnS shell.

To summarize, the sonochemical approach describes here has general validity for coating of metal nanoparticles on modified surfaces of nanotubes, nanosheets, or nanospheres. In principle, the sonochemical process described here could also be extended to other core systems like polymer spheres, where following the deposition of FePt, the polymer could be evaporated during the annealing process to generate the hollow FePt spheres. Alternative bifunctional, hybrid systems such as FePt/ZnO, or FePt/PbS, can also be attempted. Transient localized hot spots caused by ultrasonic cavitation improve the thermal decomposition of organometallic acetylacetonate precursors to form nanometer-sized FePt. Without power sonication, little FePt was formed at 120 °C in the same reaction system, which indicates that sonochemistry

(32) Zhao, Z. L.; Chen, J. S.; Ding, J.; Yi, J. B.; Liu, B. H.; Wang, J. P. *App. Phy. Lett.* **2006**, *88*, 052503.
(33) (a) Eagleton, T. S.; Searson, P. C. *Chem. Mater*. **2004**, *16*, 5027. (b) Iskandar, F.; Iwaki, T.; Toda, T.; Okuyama, K. *Nano Lett.* **2005**, *5*, 1525. (c) Duan, G.; Cai, W.; Li, Y.; Li, Z.; Cao, B.; Luo, Y. *J. Phys. Chem. B* **2006**, *110*, 7184.
(34) (a) DeLoach, L. D.; Page, R. H.; Wilke, G. D.; Payne, S. **A.**; Krupke, W. F. *IEEE J. Quantum Electron.* **1996**, *12*, 885. (b) Borse, P. H.; Deshmukh, N.; Shinde, R. F.; Date, S. K.; Kulkarni, S. K. *J. Mater. Sci*. **1999**, *34*, 6087.
(35) (a) Becker, W. G.; Bard, A. J. *J. Phys. Chem.* **1983**, *87*, 4888. (b) Chang, S.; Yoon, S, O.; Park, H. J.; Sakai, A. *Appl. Surf. Sci.* **2000**, *158*, 330. (c) Xiong, Q. H.; Chen, G.; Acord, J. D.; Liu, X.; Zengel, J. J.; Gutierrez, H. R.; Redwing, J. M.; Lew Yan Voon, L. C.; Lassen, B.; Eklund, P. C. *Nano Lett.* **2004**, *4*, 1663. (d) Rosenberga, R. A.; Shenoy, G. K.; Heigl, F.; Lee, S. T.; Kim, P. S. G.; Zhou, X. T.; Sham, T. K. *Appl. Phys. Lett.* **2005**, *86*, 263115.
(36) (a) Li, Y. J.; You, L. P.; Duan, R.; Shi, P. B.; Du, H. L.; Qiao, Y. P.; Qin, G. G. *Nanotechnology* **2004**, *15*, 581. (b) Wu, Q. Z.; Cao, H. Q.; Zhang, S. H.; Zhang, X. R.; Rabinovich, D. *Inorg. Chem.* **2006**, *45*, 7316.

has an important effect on the formation of FePt at arelatively low temperature.[13] The sonochemical deposited FePt nanoparticles have sizes of 3−5 nm, which are close to the superparamagnetic limit of FePt (4 nm), but following heat treatment, they ripened and phase-transformed to reach a stable size of ∼10 nm on the spheres and became magnetically hard by 530 °C. The geometry of the spherical surface, along with the coating of materials like ZnS or polyelectrolytes on it, serves to isolate the FePt and prevents a larger degree of sintering; therefore, an assembly of such microspheres on surfaces potentially allows for high density, three-dimensional loading of ferromagnetic nanoparticles. The chemistry developed in this work allows the FePt microspheres to form a well-packed monolayer at the solid−liquid interfac; such hydrophilic FePt microspheres could be readily transferred onto hydrophilic surfaces, where the dual magnetic−luminescence properties of the microspheres afford ready optical imaging and magnetic actuation in nanomechanical devices. The readiness of the FePt microspheres to undergo layered self-assembly on surfaces also suggests their potential to form architectured assembly of magnetic superlattices, where new collective properties due to superlattice-associated nanoscale may arise.[37]

(37) (a) Cheon, J.; Park, J.; Choi, J.; Jun, Y.; Kim, S.; Kim, M. G.; Kim, Y.; Kim, Y. J. *Proc. Natl. Acad. Sci., U.S.A.* **2006**, *103*, 3023. (b) Sra, K.; Ewers, T. D.; Xu, Q; Zandbergen H.; Schaak, R. E. *Chem. Commun.* **2006**, 750.

Conclusion

$FePt/SiO_2$ and $FePt/ZnS/SiO_2$ core−shell microspheres with a dense 3−5 nm fcc FePt coating were obtained by sonochemical reduction of platinum and iron acetylacetonates at a relatively low temperature of ∼120 °C. A novel air−liquid process could be used to self-assemble the quasi-monolayer of FePt spheres. High magnetic coercivity ($H_c \approx 12$ kOe) could be obtained for core−shell and hollow spheres after phase transition into the fct phase induced by thermal annealing. Bifunctional core−shell $FePt/ZnS/SiO_2$ and hollow FePt/ZnS spheres exhibiting both hard magnetism and luminescence have been successfully synthesized. Smaller FePt nanocrystals were obtained on ZnS-coated silica microsphere compared to polyelectrolyte-coated microsphere. The synthesized nanoparticles may have potential applications in the biomedical field and data storage.

Acknowledgment. The work was supported by National University of Singapore (NUS) academic Grant R-143-000-265-112. We thank Mr. Binghai Liu at NUS for the TEM analysis and Dr. Peng Chen at IMRE in Singapore for the photoluminescence measurements.

Supporting Information Available: Figures S1−S3. This material is available free of charge via the Internet at http://pubs.acs.org.

CM0703728